Synthesis of Ruthenium–Phosphine Complexes with Heterodiene Ligands

Olaf C. P. Beers, Michiel M. Bouman, and Cornelis J. Elsevier*

Anorganisch Chemisch Laboratorium, Universiteit van Amsterdam, Nieuwe Achtergracht 166, 1018 WV Amsterdam, The Netherlands

Wilberth J. J. Smeets and Anthony L. Spek

Bijvoet Center for Biomolecular Research, Vakgroep Kristal- en Structuurchemie, Universiteit Utrecht, Padualaan 8, 3584 CH Utrecht, The Netherlands

Received October 8, 1992

Monoazadienes (RC(H)=C(H)C(H)=NR'; MAD) react with $Ru_3(CO)_9(PPh_3)_3$ (**1**) at 115 °C in heptane to give the mononuclear complex $Ru(CO)_2(PPh_3)\{\eta^4$-RC(H)=C(H)C(H)=NR'$\}$ (**2a**, R, R' = Ph, ^{i}Pr; **2b**, R, R' = Ph, *p*-Tol). The X-ray crystal structure of **2b** has been determined, showing a distorted square pyramidal geometry with three facial sites occupied by the MAD ligand. Crystals of **2b** are monoclinic, space group $P2_1/n$, with a = 15.688(3) Å, b = 12.815(1) Å, c = 16.618(3) Å, β = 99.62(1)°, and Z = 4. Convergence was reached at R = 0.026 for 5522 reflections with $I > 2.5\ \sigma(I)$. In the case of MAD **c** (R, R' = Me, ^{i}Pr) cyclometalation and subsequent C–H activation within the R-group takes place, which leads to the formation of $Ru_2(CO)_4(PPh_3)_2\{C(H)_2CC(H)C(H)=N^iPr\}$ (**3**). The thermal fragmentation of **1** has also been examined for other heterodienes, viz. ^{i}PrN=C(H)C(H)=N^{i}Pr (^{i}Pr-DAB) and ^{i}PrN=C(Ph)C(Ph)=O (AOD). In the case of ^{i}Pr-DAB quantitative formation of $Ru(CO)_2(PPh_3)(\sigma$-*N*,σ-*N*-^{i}Pr-DAB) (**4**) occurs, whereas the product (**5**) in the case of the AOD ligand is too air-sensitive to allow characterization but is probably analogous to complex **4**. Complex **1** appears to be a convenient starting complex for the synthesis of mononuclear Ru complexes, which are generally poorly accessible. Mononuclear phosphine complexes containing cyclometalated MAD-yl ligands are prepared via opening of the halide bridge in $[Ru(CO)_2Cl\{RC=C(H)C(H)=N^iPr\}]_2$ (**a**, R = Ph; **c**, R = Me) by PPh_3 affording two isomers of $Ru(CO)_2(PPh_3)Cl\{RC=C(H)C(H)=N^iPr\}$ (**6**). Complex **6a** reacts with $NaBH_4$ to give complex **2a** in high yield, revealing that cyclometalation of MAD on $Ru(CO)_2(PPh_3)$ fragments is thermodynamically unfavorable.

Introduction

Besides their versatile coordination behavior, monoazadienes (abbreviated as MAD[1]) offer the possibility to be cyclometalated to yield a metallacycle and a metal hydride. The conditions for cyclometalation in competition with only coordination of MAD were elegantly shown in d^8-Rh and -Ir complexes by Van Baar et al.[2] In d^8-carbonyl complexes of the iron triad the conditions for cyclometalation of MAD have been less well documented. In the case of Fe only coordination complexes of MAD are known, viz. $Fe(CO)_4$(MAD), featuring a σ-N-coordinated ligand,[3] and $Fe(CO)_3$(MAD) with the ligand in the π—C=C, π—C=N bonding mode, similar to the common $Fe(CO)_3(\eta^4$-diene) complexes.[4]

In the case of Ru, the thermal reaction of MAD with $Ru_3(CO)_{12}$ has been thoroughly investigated by Mul et al. and is characterized by the cyclometalation of MAD, affording di-, tri-, and tetranuclear products.[5] The mononuclear coordination complex $Ru(CO)_3(\pi,\pi$-MAD) has never been observed in the reactions with $Ru_3(CO)_{12}$, but it can be prepared by reacting $Ru(CO)_5$ and MAD at ambient temperature.[5a] This complex appeared to be too unstable to allow purification, and in the reaction with CO at room temperature it was converted instantaneously into $Ru(CO)_5$ and uncomplexed MAD, implying the presence of a very weak bonding of MAD in $Ru(CO)_3$(MAD).

Now we present the synthesis of PPh_3-substituted Ru complexes of MAD, which we wanted to prepare in order to study the effect of the phosphine ligand on both the cyclometalation reaction of MAD and the bonding of the MAD ligand in the products. Two different approaches have been used for this purpose. Starting with the zerovalent PPh_3-substituted analogue of $Ru_3(CO)_{12}$, i.e. $Ru_3(CO)_9(PPh_3)_3$ (**1**), the tendency of MAD to be cyclometalated under thermal conditions has been studied. In the second approach mononuclear Ru(II)–phosphine complexes, containing a cyclometalated monoazadienyl ligand, have been prepared via opening of the Cl bridge in the dimer $[Ru(CO)_2Cl\{RC=C(H)C(H)=N^iPr\}]_2$ by PPh_3.[6] Substitution of the chloro ligand by a hydride then might provide $HRu(CO)_2(PPh_3)\{RC=C(H)C(H)$-N^{i}Pr$\}$, which is the theoretical product of cyclometalation of a MAD ligand on a $Ru(CO)_2(PPh_3)$ fragment. This route to the hydrido complex might allow the study of its stability, i.e. the cyclometalation equilibrium.

Finally, the thermal reaction with **1** with some other heterodienes, viz. the diazadiene ^{i}PrN=C(H)C(H)=N^{i}Pr (^{i}Pr-DAB) and the 1-aza-4-oxo-1,3-diene, ^{i}PrN=C(Ph)C(Ph)=O (AOD) have been investigated as well, in order to examine the general applicability of **1** as a starting complex for mononuclear Ru$(CO)_2(PPh_3)$ complexes of heterodienes.

Experimental Section

^{1}H, ^{13}C$\{^1$H$\}$, and ^{31}P$\{^1$H$\}$ NMR spectra were recorded on Bruker AC 100, WM 250, and AMX 300 spectrometers. The ^{13}C NMR spectra were recorded using an APT pulse sequence. IR spectra were measured on Perkin-Elmer 283 and Nicolet 7199B FTIR (liquid nitrogen cooled,

(1) Reactions of Monoazadienes with Metal Carbonyl Complexes. Part 16. For other parts see refs 5b, 6b, 27, and 33.
(2) van Baar, J. F.; Vrieze, K.; Stufkens, D. J. *J. Organomet. Chem.* **1975**, *97*, 461.
(3) Cardaci, G.; Bellachioma, G. *J. Chem. Soc., Dalton Trans.* **1976**, 1735.
(4) Otsuka, S.; Yoshida, T.; Nakamura, A. *Inorg. Chem.* **1967**, *6*, 20.
(5) (a) Mul, W. P.; Elsevier, C. J.; Polm, L. H.; Vrieze, K.; Zoutberg, M. C.; Heijdenrijk, D.; Stam, C. H. *Organometallics* **1991**, *10*, 2247. (b) Elsevier, C. J.; Mul, W. P.; Vrieze, K. *Inorg. Chim. Acta* **1992**, *200*, 689.
(6) (a) Mul, W. P.; Elsevier, C. J.; van Leijen, M.; Spaans, J. *Organometallics* **1991**, *10*, 251. (b) Beers, O. C. P.; Bouman, M. M.; Komen, A. E.; Elsevier, C. J.; Vrieze, K.; Smeets, W. J. J.; Spek, A. L. *Organometallics* **1993**, *12*, 315.

0020-1669/93/1332-3015$04.00/0

Hg, Cd, and Te detectors) spectrophotometers using matched NaCl solution cells of 0.5-mm path length. Field desorption (FD) mass spectra were obtained with a Varian MAT711 double-focusing mass spectrometer with a combined EI/FI/FD source, fitted with a 10-μm tungsten wire FD emitter containing carbon microneedles with an average length of 30 μm, using emitter currents of 0–15 mA. Elemental analyses were carried out by the Section Elemental Analysis of the Institute for Applied Chemistry, TNO Zeist, The Netherlands, or Dornis und Kolbe, Mikroanalytisches Laboratorium, Mülheim a.d. Ruhr, Germany. All preparations were carried out under an atmosphere of purified nitrogen. Carefully dried solvents were used. Silica gel for column chromatography (kieselgel 60, 70–230 mesh, E. Merck, Darmstadt, Germany) was dried before use. $Ru_3(CO)_{12}$ was used as purchased from Strem Chemicals, Inc. The monoazadienes (RC(H)=C(H)C(H)=NR', R, R' = Ph, ^{i}Pr (**a**); Ph, *p*-Tol (**b**); Me, ^{i}Pr (**c**)),[7] ^{i}Pr-DAB,[8] ^{i}PrN=C(Ph)C(Ph)=O,[9] and the complexes $Ru_3(CO)_9(PPh_3)_3$ (**1**)[10] and $[Ru(CO)_2Cl\{RC{=}C(H)C(H){=}N^iPr\}]_2$ (R = Ph, Me[6] were prepared according to literature procedures. Reported FD mass data are based on the highest peak of the isotopic pattern of the molecular ion, which corresponds to ^{102}Ru and ^{35}Cl (calculated value in parentheses).

Synthesis of $Ru(CO)_2(PPh_3)\{\eta^4$-RC(H)=C(H)C(H)=NR'} (2a, R = Ph, R' = ^{i}Pr; 2b, R = Ph, R' = *p*-Tol). The dark red suspension of 0.50 g of $Ru_3(CO)_9(PPh_3)_3$ (**1**, 0.37 mmol) and about 7 equiv of MAD **a** or **b** (**a**, R = Ph, R' = ^{i}Pr; **b**, R = Ph, R' = *p*-Tol) in 100 mL of heptane was stirred at reflux temperature for 16 h. The solvent of the resulting orange solution was evaporated and the residue chromatographed on silica. Elution with hexane and hexane/CH_2Cl_2 (1:1) afforded the complexes **2a,b**, contaminated with cinnamaldehyde, derived from silica-hydrolyzed MAD. The purification by a second chromatographic procedure with the eluent hexane/CH_2Cl_2 (1:1) and subsequent recrystallization from a saturated hexane/CH_2Cl_2 solution at –80 °C yielded the yellow air-stable complexes **2a,b** in 30–40% yield. With more polar eluents, such as CH_2Cl_2 and THF, $Ru(CO)_3(PPh_3)_2$[11] and some unidentified PPh_3-containing complexes were obtained. Crystals of **2b**, suitable for an X-ray crystal structure determination, were grown from a saturated hexane/dichloromethane solution at –30 °C. FD mass for **2a**: *m/e* 593 ($M^{\bullet+}$ = 593). Anal. Found (calcd) for $RuC_{36}H_{30}NO_2P$, **2b**: C, 67.05 (67.49); H, 5.22 (4.72); N, 2.04 (2.19); FD mass: *m/e* 641 ($M^{\bullet+}$ = 641).

Synthesis of $Ru_2(CO)_4(PPh_3)_2\{C(H)_2CC(H)C(H){=}N^iPr\}$ (3). The dark red suspension of 0.50 g of $Ru_3(CO)_9(PPh_3)_3$ (**1**, 0.37 mmol) and about 7 equiv of MAD **c** (R = Me, R' = ^{i}Pr) in 100 mL of heptane was stirred at reflux for 16 h. The solvent of the resulting orange solution was evaporated and the residue chromatographed on silica. Elution with hexane/CH_2Cl_2 (1:1) afforded complex **3**, contaminated with $Ru(CO)_3(PPh_3)_2$.[11] The latter was selectively precipitated from a diluted hexane/dichloromethane solution at –80 °C. Complex **3** was obtained as air-stable orange microcrystalline needles in 0.26-g yield (25%) by crystallization from the concentrated supernatant liquor at –30 °C. With more polar eluents, such as CH_2Cl_2 and THF, some unidentified PPh_3-containing complexes were obtained. Anal. Found (calcd) for $Ru_2C_{47}H_{41}NO_4P_2$, **3**: C, 58.54 (59.55); H, 4.42 (4.36); N, 1.48 (1.48); P, 5.66 (6.54). [Some CH_2Cl_2 is present from crystallization, for **3**·0.25CH_2Cl_2 calcd C, 58.43; H, 4.27; N, 1.44; P, 6.39.] FD mass: *m/e* 949 ($M^{\bullet+}$ = 949).

Synthesis of $Ru(CO)_2(PPh_3)\{^iPrN{=}C(H)C(H){=}N^iPr\}$ (4). A suspension of 0.50 g of $Ru_3(CO)_9(PPh_3)_3$, **1** (0.37 mmol), and 0.36 g of ^{i}Pr-DAB (2.6 mmol, 7 equiv) in 50 mL of heptane was refluxed for 16 h. The resulting deep-purple, extremely air-sensitive, hot reaction mixture was filtered. The filtrate then was cooled to –78 °C, and complex **4** was allowed to precipitate. After decanting of the supernatant liquor, pure **4** was obtained as an air-sensitive dark red powder in about 0.40-g yield (65%). The yield of **4** before precipitation was estimated to be 95% on the basis of IR spectroscopy. FD mass for **4**: *m/e* 560 ($M^{\bullet+}$ = 560).

Synthesis of $Ru(CO)_2(PPh_3)\{^iPrN{=}C(Ph)C(Ph){=}O\}$ (5). A suspension of 0.50 g of $Ru_3(CO)_9(PPh_3)_3$ (**1**, 0.37 mmol) and 0.65 g of ^{i}PrN=C(Ph)C(Ph)=O (2.6 mmol, 7 equiv) in 50 mL of heptane was refluxed for 16 h. The resulting deep-purple, extremely air-sensitive, hot reaction mixture was filtered. Attempts to precipitate **5** from the filtrate failed. Complex **5** appeared to be too air-sensitive to allow characterization by spectroscopic techniques.

Synthesis of $Ru(CO)_2Cl(PPh_3)\{RC{=}C(H)C(H){=}N^iPr\}$ (6a, R = Ph; 6c, R = Me). Method I. A solution of 0.3 mmol of $[Ru(CO)_2Cl\{RC{=}C(H)C(H){=}N^iPr\}]_2$ and 0.16 g of PPh_3 (0.6 mmol, 2 equiv) in 50 mL of hexane was stirred at 60 °C. After 10 min, a white-yellow precipitate was formed and the reaction was stopped. The reaction mixture was chromatographed on silica. Elution with hexane/diethyl ether (9:1) yielded a small amount of unreacted parent complex. With hexane/diethyl ether (1:1) the yellow air-stable complex **6** was eluted in 55–65% yield. Subsequent elution with THF yielded a small amount of $Ru(CO)(PPh_3)_2Cl\{RC{=}C(H)C(H){=}N^iPr\}$. Complexes **6a,c** were formed in two isomers **A** and **B** (Figure 3) in the ratio 1:3 for **6a** and 1:2 for **6c**. FD mass: **6a**, *m/e* 628 ($M^{\bullet+}$ = 628); for **6c**, *m/e* 566 ($M^{\bullet+}$ = 566).

Method II. When the same reaction was performed at 25 °C during 3 h, **6a,c** were formed in about 80% yield and the ratio **A**:**B** now was 2:1 for **6c**, while **6a** was formed only in form **A**.

Method III. Using $Ru(CO)_3Cl\{RC{=}C(H)C(H){=}N^iPr\}$ as the starting complex, instantaneous gas formation was observed when PPh_3 was added in CH_2Cl_2 solution. The isomer ratio **A**:**B** was the same as under method II.

Isomerization of Complex 6. A small amount of **6a**, pure isomer **A** (60 mg, 0.1 mmol), was dissolved in 20 mL of heptane, and the mixture was stirred at 100 °C. After 2 h a white-yellow precipitate was formed. The supernatant liquid was examined with ^{1}H and ^{31}P NMR and showed an isomer ratio **A**:**B** of 3:1. The precipitate was analyzed by ^{31}P NMR (17.7 and 21.0 ppm, singlets), ^{1}H NMR (7.9–7.1 ppm, multiplet), and FD mass (isotope patterns at *m/e* 960–970 and 830 (M – CO)/600 (M – PPh_3)), as a mixture of $Ru_2(CO)_6(PPh_3)_2Cl_2$ ($M^{\bullet+}$ = 966) and $Ru(CO)(PPh_3)_2Cl\{PhC{=}C(H)C(H){=}N^iPr\}$ ($M^{\bullet+}$ = 858), respectively, formed in a ratio of about 5:1.

Conversion of 6a into 2a. An excess of $NaBH_4$ (0.1 g, ca. 10 equiv) was added at –30 °C to a solution of 0.18 g of **6a** (0.3 mmol), pure isomer **A**, in 20 mL of dichloromethane. After being stirred for 2.5 h, the suspension was allowed to warm to ambient temperature gradually. After the addition of 20 mL of hexane, the excess of $NaBH_4$ was removed by filtration. The filtrate was purified by column chromatography on silica. Elution with hexane/CH_2Cl_2 (1:1) yielded 0.12 g of complex **2a** (70%).

Crystal Structure Determination of 2b. X-ray data were collected ($\omega/2\theta$-scan; $\Delta\omega = 0.70 + 0.35 \tan\theta$°; $\theta_{min,max}$ = 1.24, 27.47°; *h*, 0 to 20, *k*, 0 to 16, *l*, –21 to 20) on an Enraf-Nonius CAD4 diffractometer (Mo Kα, Zr filtered, λ = 0.710 73 Å) for a yellow block-shaped crystal mounted on top of a glass fiber. Unit cell parameters were determined from a least-squares treatment of the SET4 setting angles of 25 reflections in the range $14.1 < \theta < 19.2$°. The unit cell parameters were checked for the presence of higher lattice symmetry.[12] The intensities of 7420 reflections were corrected for Lp and for a linear decay (3%) of the intensity control reflections during the 121 h of X-ray exposure time but not for absorption and merged into a unique set of 5522 observed reflections with $I > 2.5\sigma(I)$. The structure was solved with direct methods (SHELXS86[13]) and a series of subsequent difference Fourier analyses. Refinement on *F* was carried out by full matrix least-squares techniques. H atoms were introduced on calculated positions (C–H = 0.98 Å) and included in the refinement riding on their carrier atoms. All non-H atoms were refined with anisotropic thermal parameters, and H-atoms with one common isotropic thermal parameter (U = 0.0246(12) Å^2). A hexane solvate molecule, located around an inversion center, could not be located from difference Fourier maps unambiguously and was taken into account in the structure factor and refinement calculations by direct Fourier transformation of the electron density in the cavity, following the BYPASS procedure.[14] Weights were introduced in the final refinement cycles, and convergence was reached at R = 0.0260. Crystal data are collected in Table I, and positional parameters are listed in Table II. Neutral-atom scattering factors were taken from ref 15 and corrected for anomalous dispersion.[16] All calculations were performed with SHELX76[17] and PLATON[18] (geometrical calculations and illustrations) on a MicroVax-II cluster.

(7) Barany, H. C.; Braude, E. A.; Pianka, M. *J. Chem. Soc.* **1949**, 1898.
(8) Bock, H.; tom Dieck, H. *Chem. Ber.* **1967**, *100*, 228.
(9) Wheatley, W. B.; Fitzgibbon, W. E.; Cheney, Lee C. *J. Org. Chem.* **1953**, *18*, 1564.
(10) Piacenti, F.; Bianchi, M.; Benedetti, E.; Sbrana, G. *J. Inorg. Nucl. Chem.* **1967**, *29*, 1389.
(11) L'Eplattenier, F.; Calderazzo, F. *Inorg. Chem.* **1968**, *7*, 1290.
(12) Spek, A. L. *J. Appl. Crystallogr.* **1988**, *21*, 578.
(13) Sheldrick, G. M. SHELXS86. Program for crystal structure determination. University of Göttingen, Federal Republic of Germany, 1986.
(14) van der Sluis, P.; Spek, A. L. *Acta Crystallogr.* **1990**, *A46*, 194.
(15) Cromer, D. T.; Mann, J. B. *Acta Crystallogr.* **1968**, *A24*, 321.
(16) Cromer, D. T.; Liberman, D. *J. Chem. Phys.* **1970**, *53*, 1891.
(17) Sheldrick, G. M. SHELX76. Crystal structure analysis package. University of Cambridge, England, 1976.
(18) Spek, A. L. *Acta Crystallogr.* **1990**, *A46*, C34.

Table I. Crystal Data for Complex **2b**

chem formula	$C_{36}H_{30}NO_2PRu\cdot{}^1/_2C_6H_{14}$	λ, Å	0.710 73
fw	683.77	space group	$P2_1/n$ (No. 14)
a, Å	15.688(3)	Z	4
b, Å	12.815(1)	D_x, g cm^{-3}	1.379
c, Å	16.618(3)	μ, cm^{-1}	5.5
β, deg	99.62(1)	R^a	0.0260
V, Å^3	3293.9(9)	$R_w{}^b$	0.0320
λ, Å	0.710 73		

^{a} $R = \Sigma(|F_o| - |F_c|)/\Sigma|F_o|$. ^{b} $R_w = \{\Sigma w(|F_o| - |F_c|)^2/\Sigma w|F_o|^2\}^{1/2}$.

Table II. Final Coordinates and Equivalent Isotropic Thermal Parameters of the Non-Hydrogen Atoms of **2b**

atom	x	y	z	U(eq)^a (Å^2)
Ru	0.096 91(1)	0.371 89(1)	0.333 45(1)	0.0122(1)
P	0.055 83(3)	0.416 93(4)	0.193 82(3)	0.0127(2)
O(1)	−0.015 26(11)	0.179 66(13)	0.325 14(10)	0.0275(6)
O(2)	0.248 16(11)	0.222 64(14)	0.330 09(10)	0.0275(5)
N	0.177 74(11)	0.506 45(14)	0.377 42(11)	0.0154(5)
C(1)	−0.086 47(14)	0.465 23(18)	0.365 81(14)	0.0199(7)
C(2)	−0.143 84(15)	0.533 5(2)	0.318 47(15)	0.0252(8)
C(3)	−0.232 42(16)	0.512 1(2)	0.301 97(17)	0.0343(9)
C(4)	−0.264 38(16)	0.422 4(2)	0.332 40(18)	0.0365(9)
C(5)	−0.209 10(16)	0.355 4(2)	0.381 43(16)	0.0314(8)
C(6)	−0.121 05(15)	0.376 7(2)	0.398 56(14)	0.0248(7)
C(7)	0.007 13(14)	0.485 81(18)	0.377 35(13)	0.0182(7)
C(8)	0.066 60(14)	0.444 16(18)	0.444 61(13)	0.0181(7)
C(9)	0.155 67(14)	0.458 69(17)	0.444 36(13)	0.0177(6)
C(10)	0.266 82(14)	0.516 35(16)	0.373 01(13)	0.0155(6)
C(11)	0.328 12(14)	0.545 62(17)	0.440 76(13)	0.0176(6)
C(12)	0.413 98(14)	0.559 83(17)	0.432 56(13)	0.0178(6)
C(13)	0.442 37(13)	0.545 53(16)	0.358 48(13)	0.0159(6)
C(14)	0.380 79(14)	0.517 71(17)	0.291 42(14)	0.0178(6)
C(15)	0.294 65(14)	0.503 56(17)	0.298 48(13)	0.0175(6)
C(16)	0.535 89(14)	0.559 51(18)	0.350 01(14)	0.0189(7)
C(17)	0.025 72(14)	0.254 09(18)	0.327 06(13)	0.0180(7)
C(18)	0.191 75(14)	0.279 84(18)	0.329 27(13)	0.0182(7)
C(19)	−0.036 68(14)	0.347 59(16)	0.136 43(13)	0.0149(6)
C(20)	−0.111 08(14)	0.336 86(18)	0.172 31(14)	0.0184(7)
C(21)	−0.185 57(14)	0.293 91(18)	0.127 88(15)	0.0218(7)
C(22)	−0.186 82(15)	0.259 92(18)	0.048 75(14)	0.0220(7)
C(23)	−0.112 96(15)	0.268 16(18)	0.013 49(14)	0.0209(7)
C(24)	−0.038 31(14)	0.312 63(17)	0.057 55(13)	0.0178(6)
C(25)	0.075 37(14)	0.631 33(17)	0.218 67(13)	0.0180(6)
C(26)	0.053 24(15)	0.735 90(18)	0.206 36(14)	0.0223(7)
C(27)	−0.021 16(15)	0.763 82(19)	0.153 73(15)	0.0240(8)
C(28)	−0.074 28(15)	0.687 21(18)	0.113 48(14)	0.0224(7)
C(29)	−0.052 61(14)	0.582 38(18)	0.124 99(13)	0.0178(6)
C(30)	0.022 38(14)	0.553 58(17)	0.177 21(13)	0.0152(6)
C(31)	0.141 16(13)	0.401 37(17)	0.131 55(12)	0.0138(6)
C(32)	0.184 92(14)	0.305 65(17)	0.134 00(13)	0.0162(6)
C(33)	0.254 67(15)	0.293 80(18)	0.093 63(14)	0.0209(7)
C(34)	0.281 63(15)	0.376 59(19)	0.049 93(14)	0.0235(7)
C(35)	0.237 53(15)	0.471 14(19)	0.046 08(14)	0.0230(7)
C(36)	0.167 53(14)	0.483 46(18)	0.086 87(13)	0.0181(7)

^{a} U(eq) = $^1/_3$ of the trace of the orthogonalized U tensor.

Results

Formation of the Complexes. The thermal reaction of the monoazadienes **a** (R, R′ = Ph, ^{i}Pr) and **b** (R, R′ = Ph, *p*-Tol) with $Ru_3(CO)_9(PPh_3)_3$ (**1**) resulted in the fragmentation of the cluster into the mononuclear complexes **2a,b** in moderate yields (Figure 1) concomitant with the formation of considerable amounts of $Ru(CO)_3(PPh_3)_2$[11] and some unidentified RuP complexes. The spectroscopic data of **2a,b** indicate that the monoazadiene ligand is present in the π,π-coordination mode as confirmed for **2b** by an X-ray crystal structure determination (vide infra).

In the case of MAD **c** (R, R′ = Me, ^{i}Pr) the thermal reaction with **1** took another course, which is expressed by the formation of complex **3** (Figure 1). Complex **3**, which was structurally characterized on the basis of spectroscopic data (vide infra), possesses a five-membered metallacycle which is dehydrogenated at the R substituent (Me group), resulting in an "allyl–imine"

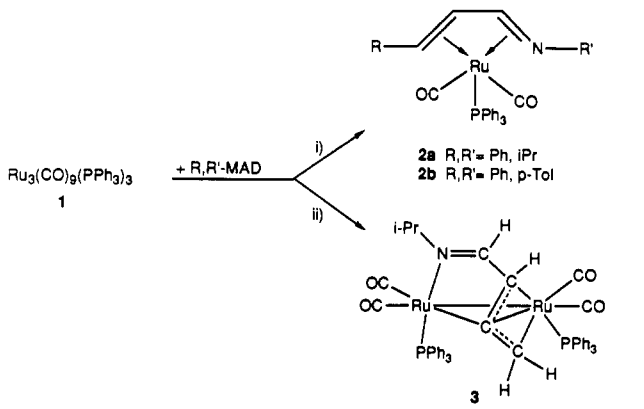

Figure 1. Reactivity of $Ru_3(CO)_9(PPh_3)_3$ (**1**) with monoazadienes: (i) R, R′ = Ph, ^{i}Pr (**a**) or Ph, *p*-Tol (**b**); (ii) R, R′ = Me, ^{i}Pr.

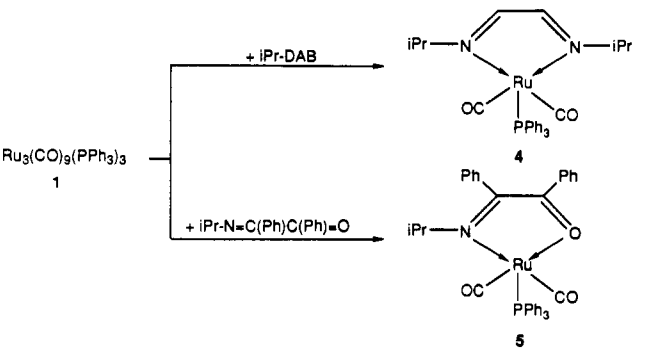

Figure 2. Reactivity of **1** toward a diazadiene (^{i}Pr-DAB) and an azaoxadiene.

type of ligand system. The allyl part is η^3-coordinated to the nonmetalated $Ru(CO)_2(PPh_3)$ moiety.

In order to examine whether the fragmentation of **1** into mononuclear complexes can be applied more generally, the thermal reaction of **1** with a 1,4-diaza-1,3-diene (^{i}Pr-DAB) and a 1-aza-4-oxo-1,3-diene (AOD, ^{i}PrN = C(Ph)C(Ph)=O) was attempted as well. In both cases an extremely air-sensitive, deep-purple colored solution was obtained. Only in the case of ^{i}Pr-DAB could the product, formed in almost quantitative yields, be completely characterized by IR, NMR, and FD mass spectroscopy as the mononuclear complex $Ru(CO)_2(PPh_3)$(^{i}Pr-DAB) (**4**).

In the case of the AOD ligand the extreme air-sensitivity of the product precluded the workup of the reaction mixture under nitrogen atmosphere using normal Schlenk techniques and subsequent characterization of the product by spectroscopy. Both the color and its oxidation properties toward air, however, point to a chelating AOD ligand coordinated to a $Ru(CO)_2(PPh_3)$ fragment (see **5** in Figure 2).

In order to obtain more information about the thermal stability of the theoretical cyclometalation product of MAD on a $Ru(CO)_2(PPh_3)$ fragment, i.e. $HRu(CO)_2(PPh_3)$\{RC=C(H)C(H)=NR′\}, an alternative reaction route to this complex was attempted which allowed milder reaction conditions. Reaction of the known halogen-bridged complex $[Ru(CO)_2Cl\{RC{=}C(H)C(H){=}N^iPr\}]_2$[9] with PPh_3 at 60 °C during 10 min resulted in the formation of $Ru(CO)_2(PPh_3)Cl\{RC{=}C(H)C(H){=}N^iPr\}$ (**6**), which was formed as a mixture of two isomers **A** and **B** (Figure 3). The structural data of these isomers will be discussed below. In the case of **6a**, isomer **A** could be obtained selectively when milder reaction conditions (25 °C, 1 h) were applied. Under these conditions **6c** was formed with the ratio **A**:**B** of 2:1.

Complex **6a** (isomer **A**) isomerized thermally into a mixture of **A** and **B**. During this reaction a byproduct precipitated, which appeared to be free of MAD-yl and showed a resonance at 17.7 ppm in the ^{31}P-NMR spectrum. The same product was also

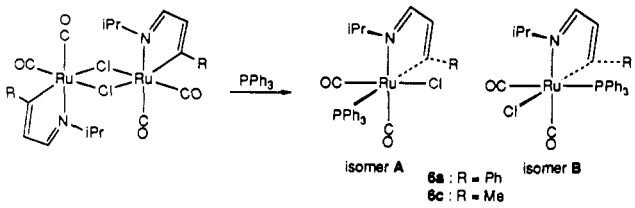

Figure 3. Formation of **6**, which exists in two isomers, **A** and **B**.

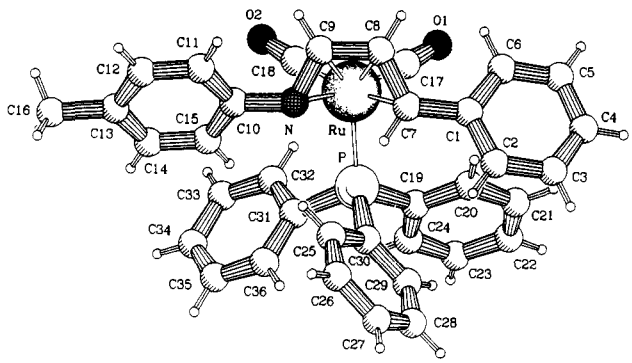

Figure 4. Molecular structure of $Ru(CO)_2(PPh_3)\{\eta^4$-PhC(H)=C(H)C(H)=N-*p*-Tol$\}$ (**2b**).

formed in the reaction of **1** with CCl_4 and probably has the formula $[Ru(CO)_3(PPh_3)Cl]_2$,[19] according to its FD mass spectrum.

Finally, complex **6a** (isomer **A**) was reacted with $NaBH_4$ in order to exchange the Cl ligand by a hydride ligand. This reaction resulted in the formation of complex **2a** in good yields, indicating that the hypothetical product $HRu(CO)_2(PPh_3)$(MAD-yl) undergoes fast reductive elimination to give $Ru(CO)_2(PPh_3)$ and MAD, which form together **2a**.

Molecular Structure of 2b. The molecular geometry of **2b** is shown in Figure 4, and selected bond distances and angles are given in Table III. The monoazadiene ligand in **2b** is η^4-coordinated to the $Ru(CO)_2(PPh_3)$ moiety with all bonded atoms approximately equidistant from the metal (2.189(2)–2.24(2) Å). The central C–C bond (C(8)–C(9) = 1.410(3)) of the coordinated heterodiene is even shorter than the outer C–C bond (C(7)–C(8) = 1.434(3)), which has also been observed in $Fe(CO)_2PR_3$ complexes of π,π-coordinated benzylideneacetone (BDA).[21] This feature points to a significant amount of π-back-bonding from the metal fragment to the antibonding orbital of the heterodiene. The intraligand distances C(8)–C(9) and C(7)–C(8) in **2b** also compare very well with the corresponding distances in $Fe(CO)_3\{\eta^4$-PhC(H)=C(H)C(H)=NPh$\}$ (1.413(7) and 1.433(9) Å, respectively[11]). So the effect exerted by a $Fe(CO)_3$ and a $Ru(CO)_2(PPh_3)$ fragment on a π,π-coordinated monoazadiene is very similar, implying a comparable bond strength in both complexes. The plane of the phenyl group (R) makes an angle of 31.10(14)° with the C(7)–C(8)–C(9)–N plane, while the plane of the *p*-Tol group (R′) makes an angle of –40.43(13)°, indicating a reduced π-overlap of both substituents with the heterodiene π-system. A similar effect but less pronounced (mean values of angles = 19 and –36°, respectively[22] was observed in the $Fe(CO)_3$ analogue of **2b**. The larger twist of the R and R′ group with respect to the plane of the heterodiene in **2b** may be induced by crystal packing effects or by the large steric requirements of the PPh_3 group.

The angles P–Ru–X with X = C(7), N, C(17), and C(18) (94.44(6), 100.48(5), 94.52(7), and 101.57(7)°, respectively) are all close to 90°, and therefore the geometry of **2b** can best be described as distorted octahedral with three facial sites occupied by the MAD ligand. In this description the C(8)–C(9) bond occupies the axial position, trans to the PPh_3 group. This geometry is completely comparable to the structure of $Fe(CO)_2(PPh_3)$(BDA)[21] and also to the geometry in the $Fe(CO)_3$ analogue of **2b** (corresponding angles in the latter = 93.4(3), 97.2(3), 97.2(3), and 102.4(3)°, respectively[22]), showing that the steric bulk of the PPh_3 group does not effect the geometry of the complex.

Spectroscopy. The spectroscopic data of the four types of complexes have been listed in the Tables IV–VI. The coordination mode of the heterodiene ligand in each of these types will be discussed now.

$Ru(CO)_2(PPh_3)(\eta^4$-R,R′-MAD) (2a,b). The IR spectrum of **2** shows two sharp absorption bands in the carbonyl area, as can be expected when **2** is present as one isomer. In the NMR spectra one set of resonances is observed even at low temperature, which also points to a static molecule in one isomeric form. This feature is in contrast to the behavior of $Fe(CO)_3(\pi,\pi$-MAD), in which the CO ligands are involved in a rapid scrambling process at room temperature on the NMR time scale.[23] In the literature there is some contradiction about the dynamic behavior of the analogous $Fe(CO)_2(PR_3)(\eta^4$-BDA) complexes, featuring a π,π-coordinated monooxadiene and possessing a strikingly similar solid-state structure compared to that of **2b** (vide supra). Vichi et al. have reported that $Fe(CO)_2(PR_3)(\eta^4$-BDA) is not fluxional,[24,25] whereas Howell et al. have described its dynamic behavior on the basis of NMR data.[26] No dynamic process has been observed in the case of the Ru(MAD) complex **2**.

The coupling constants $J(P,H_{im})$, $J(P,H_\alpha)$, and $J(P,H_\beta)$ vary between 3.0 and 8.4 Hz and are in agreement with the molecular geometry of the solid-state structure. Coupling with ^{31}P has been observed on just one CO ligand in **2**, which is probably C(18) as the angle P–Ru–C(18) (100.57(7)°) deviates more from 90° than the angle P–Ru–C(17) (94.52(7)°).

The chemical shifts of H_{im}/C_{im} (±6.7/107 ppm), H_α/C_α (±5.4/77 ppm), and H_β/C_β (±2.1/66 ppm) are completely comparable to the corresponding data for $Fe(CO)_3(\eta^4$-MAD)[4,23] and thus confirm the π,π-coordination mode of MAD in **2**.

$Ru_2(CO)_4(PPh_3)_2(C(H)_2CC(H)C(H)=N^iPr)$ (3). The structure of complex **3** has been determined solely on the basis of the spectroscopic and analytical data. The FD mass spectrum of **3** (*m/e* 949) corresponds to a $Ru_2(CO)_4(PPh_3)_2$ skeleton with a dehydrogenated monoazadienyl ligand (MAD – 2H). The $^{31}P\{^1H\}$ NMR spectrum shows two doublets at 48.0 and 46.1 ppm ($J(P,P)$ = 27 Hz), which, together with the small coupling constants on the ^{13}C NMR resonances of the carbonyl ligands ($J(P,C)$ in the range 4–10 Hz), points to a $(CO)_2(PPh_3)RuRu(PPh_3)(CO)_2$ skeleton.

The assignment of the proton resonances of **3** was facilitated by a *J*-resolved ^1H-NMR spectrum, which allowed the distinction between H- and P-couplings (see Table V). The resonance of H_{im} is masked by the proton resonances of the PPh_3 groups, but the chemical shift of C_{im} at 172.0 ppm is indicative for an imine moiety which is not π-coordinated. Besides the Me resonances of the ^{i}Pr group, no other Me resonance is present. Instead, two resonances at 2.47 and 2.22 ppm are observed, which point to a CH_2 group derived from a partially dehydrogenated Me substituent. The resonances of H_α/C_α at 3.75/75.1 ppm are indicative for a π-coordinated olefinic moiety.

These NMR data of the coordinated organic ligand in **3** compare reasonably well to the data of $MRu(CO)_6(C(H)_2CC$-

(19) The reaction of **1** with CCl_4 has been reported earlier,[20] and the product was analyzed as $[Ru(CO)_2(PPh_3)Cl_2]_2$.
(20) Johnson, B. F. G.; Johnston, R. D.; Lewis, J. *J. Chem. Soc. A* **1969**, 792.
(21) Vichi, E. J. S.; Raithby, P. R.; McPartlin, M. *J. Organomet. Chem.* **1983**, *256*, 111.
(22) (a) de Cian, A.; Weiss, R. *J. Chem. Soc., Chem. Commun.* **1968**, 348. (b) de Cian, A.; Weiss, R. *Acta Crystallogr.* **1972**, *B28*, 3264.
(23) Leibfritz, D.; tom Dieck, H. *J. Organomet. Chem.* **1976**, *105*, 255.
(24) Vichi, E. J. S.; Fujiwara, F. Y.; Stein, E. *Inorg. Chem.* **1985**, *24*, 286.
(25) Calhorda, M. J.; Vichi, E. J. S. *Organometallics* **1990**, *9*, 1060.
(26) Howell, J. A. S.; Dixon, D. T.; Kola, J. C. *J. Organomet. Chem.* **1984**, *266*, 69.

Table III. Selected Bond Distances (Å) and Bond Angles (deg) of **2b** (with Esd's in Parentheses)

		Bond Distances			
Ru–P	2.377(7)	Ru–N	2.1922(18)	Ru–C(7)	2.234(2)
Ru–C(8)	2.189(2)	Ru–C(9)	2.217(2)	Ru–C(17)	1.870(2)
Ru–C(18)	1.909(2)	P–C(19)	1.828(2)	P–C(30)	1.836(2)
P–C(31)	1.835(2)	O(1)–C(17)	1.148(3)	O(2)–C(18)	1.147(3)
N–C(9)	1.364(3)	N–C(10)	1.417(3)	C(7)–C(8)	1.434(3)
C(8)–C(9)	1.410(3)				
		Bond Angles around Ru			
P–Ru–N	100.48(5)	P–Ru–C(7)	94.44(6)	P–Ru–C(8)	131.34(6)
P–Ru–C(9)	134.26(6)	P–Ru–C(17)	94.52(7)	P–Ru–C(18)	101.57(7)
N–Ru–C(7)	74.83(7)	N–Ru–C(8)	65.23(8)	N–Ru–C(9)	36.04(7)
N–Ru–C(17)	163.84(8)	N–Ru–C(18)	95.01(8)	C(7)–Ru–C(8)	37.82(8)
C(7)–Ru–C(9)	66.29(8)	C(7)–Ru–C(17)	98.22(9)	C(7)–Ru–C(18)	162.44(9)
C(8)–Ru–C(9)	37.33(8)	C(8)–Ru–C(17)	100.23(9)	C(8)–Ru–C(18)	124.95(9)
C(9)–Ru–C(17)	127.84(9)	C(9)–Ru–C(18)	97.01(9)	C(17)–Ru–C(18)	87.75(10)
		Bond Angles in Ligand Part			
C(9)–N–C(10)	117.98(18)	Ru–C(7)–C(1)	120.65(16)	Ru–C(7)–C(8)	69.37(13)
C(1)–C(7)–C(8)	122.7(2)	Ru–C(8)–C(7)	72.81(12)	Ru–C(8)–C(9)	72.44(13)
C(7)–C(8)–C(9)	117.7(2)	Ru–C(9)–N	70.98(12)	Ru–C(9)–C(8)	70.23(12)
N–C(9)–C(8)	116.64(19)	N–C(10)–C(11)	122.11(19)	N–C(10)–C(15)	119.66(19)
Ru–C(17)–O(1)	177.2(2)	Ru–C(18)–O(2)	176.88(19)		

Table IV. IR and ^{31}P-NMR Data for $Ru(CO)_2(PPh_3)\{\eta^4$-RC(H)=C(H)C(H)=NR'} (**2a,b**), $Ru_2(CO)_4(PPh_3)_2\{C(H)_2CC(H)C(H)=N^iPr\}$ (**3**), $Ru(CO)_2(PPh_3)\{^iPrN=C(H)C(H)=N^iPr\}$ (**4**), and $Ru(CO)_2(PPh_3)Cl\{RC=C(H)C(H)=NR'\}$ (**6a,6c**) (**a**, R = Ph, R' = ^{i}Pr; **b**, R = Ph, R' = *p*-Tol; **c**, R = Me, R' = ^{i}Pr)

	ν(CO)[a] (cm^{-1})	δ[b] (ppm)
2a	2007(s), 1945(s)	31.8
2b	2013(s), 1954(s)	34.0
3	2008(vs), 1968(m), 1943(s)	48.0 (d, 27), 46.1 (d, 27)
4	1976(s), 1915(s)	37.2
6a, A	2045(s), 1976(s)	12.6
6a, B	2045(s), 1976(s)	23.7
6c, A	2039(s), 1972(s)	11.8
6c, B	2051(s), 1972(s)	21.9

[a] IR data of hexane solutions. [b] ^{31}P-NMR data in $CDCl_3$, at 120 MHz, 293 K, δ relative to 85% H_3PO_4, positive shifts to high frequency.

(H)C(H)=N^{i}Pr) (M = Fe,[27] M = Ru[28]), in which the ligand is in the so called "allyl–imine" coordination mode, and therefore the same mode is assigned to the ligand system in **3** (see Figure 1).

$Ru(CO)_2(PPh_3)(^iPrN=C(H)C(H)=N^iPr)$ (4). FD mass spectroscopy appeared to be an excellent tool for the identification of the extremely air-sensitive complex **4**. The spectrum showed an isotopic pattern at *m/e* 560, corresponding to the mononuclear species $Ru(CO)_2(PPh_3)(^i$Pr-DAB). The IR spectrum showed, as expected, two absorption bands in the terminal CO-stretching area at 1976 and 1915 cm^{-1}. These values are about 30 cm^{-1} lower than those of complex **2**, indicating that the electron density at Ru in **4** is larger, due to the inferior electron-accepting properties of a σ-N-, σ-N-coordinated DAB ligand as compared to a π,π-coordinated MAD ligand.

Both the ^{1}H and ^{13}C NMR spectra of **4** were recorded at two different magnetic field strengths, allowing the distinction between signals coupled to the ^{31}P nucleus and uncoupled signals. Both the ^{1}H and ^{13}C NMR spectra of **4** show one signal for the imine moiety and one signal for the methine of the ^{i}Pr group pointing to the presence of a single isomer of **4** featuring a symmetrically bonded ^{i}Pr-DAB ligand. This observation leaves only one possible geometry for **4**, viz. a square pyramidal structure with the PPh_3 ligand occupying the apical position. Such a square pyramidal geometry has been found before in the crystal structure of Fe-$(CO)_3\{2,6\text{-}(iPr)_2C_6H_3\text{-DAB}\}$.[29] This molecular geometry also accounts for the small couplings with ^{31}P observed at H_{im} (J(H,P) = 5.9 Hz), at the methine resonances of the ^{i}Pr group (J(C,P) = 3.8 Hz; J(H,P) = 1.9 Hz) and at the carbonyl ligands (J(C,P) = 5.9 Hz).

As the reduced number of resonances observed for the carbonyls and the DAB ligand at 293 K could also be a result of a dynamic process involving Berry pseudorotations, the ^{1}H and ^{13}C NMR spectra of **4** were recorded at 223 K as well. At this temperature no change with respect to the spectra at 293 K was observed, thus making the occurrence of a dynamic process in **4** less likely.

$Ru(CO)_2(PPh_3)Cl\{RC=C(H)C(H)=N^iPr\}$ (6a, R = Ph; 6c, R = Me). As mentioned before, complex **6** exists as two isomers, **A** and **B**. The coupling of the P nucleus and the C/H nuclei of the monoazadienyl ligand allow the almost complete assignment of the molecular geometry of both isomers.

In the case of **6a** (isomer **A**), which could be prepared in pure form, a large coupling (76 Hz) is present on the resonance of C_β at 211.4 ppm, pointing to a mutual trans arrangement of PPh_3 and C_β. Together with the clearly separated CO stretching vibrations in the IR spectrum, which is indicative for a cis arrangement of the carbonyl ligands, the geometry of isomer **A** is determined as depicted in Figure 3.

For isomer **B** of **6a,c**, a large ^2J(P,C) (±98 Hz) was observed on one of the CO ligands, pointing to the mutual trans arrangement of one CO ligand and PPh_3, whereas $J(P,C_\beta)$ of 8–9 Hz is in agreement with the cis geometry of PPh_3 and C_β. The positions of the other CO ligand and the Cl atom cannot be deduced from the spectroscopic data. The geometry of isomer **B** as shown in Figure 3 is plausible by using the same arguments as used for the assignment of the structure of the parent complex $[Ru(CO)_2X\{RC=C(H)C(H)=N^iPr\}]_2$,[6] viz. the better donor atom of the monoazadienyl ligand (i.e. the N-atom) will be in trans position to the better acceptor (i.e. CO).

The chemical shifts of the ligands in **6a,c** are completely comparable to those of $Ru(CO)_3Cl\{RC=C(H)C(H)=N^iPr\}$; for a discussion of these data see ref 6.

Discussion

Fragmentation of $Ru_3(CO)_9(PPh_3)_3$ (1) in the Presence of Heterodienes. In contrast to its all-carbonyl analogue $Ru_3(CO)_{12}$, the triangular complex $Ru_3(CO)_9(PPh_3)_3$ (**1**) has found very limited application in the synthesis of organometallic complexes. The kinetics of the substitution and fragmentation reactions of

(27) Beers, O. C. P.; Elsevier, C. J.; Vrieze, K.; Smeets, W. J. J.; Spek, A. L. *Organometallics*, in press.
(28) Polm, L. H.; Elsevier, C. J.; Mul, W. P.; Vrieze, K.; Christophersen, M. J. N.; Muller, F.; Stam, C. H. *Polyhedron* **1988**, *7*, 2521.
(29) Kokkes, M. W.; Stufkens, D. J.; Oskam, A. *J. Chem. Soc., Dalton Trans.* **1984**, 1005.

Table V. ^{1}H-NMR Data[a] for $Ru(CO)_2(PPh_3)\{\eta^4$-RC(H)=C(H)C(H)=NR'$\}$ (**2a,b**), $Ru_2(CO)_4(PPh_3)_2\{C(H)_2C(H)C(H)=N^iPr\}$ (**3**), $Ru(CO)_2(PPh_3)\{^iPrN=C(H)C(H)=N^iPr\}$ (**4**), and $Ru(CO)_2(PPh_3)Cl\{RC=C(H)C(H)=NR'\}$ (**6a,6c**) (**a**, R = Ph, R' = ^{i}Pr; **b**, R = Ph, R' = *p*-Tol; **c**, R = Me, R' = ^{i}Pr)

	H_{im}	H_α	H_β	R + PPh_3	R'
2a	6.59 (dd, *3.0* 3.3)	5.37 (ddd, 3.4, *3.4*, 8.4)	2.05 (dd, 8.4, *8.4*)	6.40, 7.45–6.98 (m)	2.14 (sept, 6.3), 1.18/0.56 (d, 6.3)
2b	6.93 (dd, 3.0, *3.0*)	5.54 (ddd, 3.2, *3.2*, 8.5)	2.12 (dd, *8.4*, 8.5)	6.46, 7.42–6.98 (m)	6.67 (d, 8.3), 6.35 (d, 8.3), 2.16 (s)
3	*c*	3.75 (s, br)		2.47 (d, *14.1*), 2.22 (dd, *9.7*, 1.8), 7.58–7.36 (m)	3.11 (sept, 6.5), 1.04/0.31 (d, 6.5)
4[b]	7.32 (d, *5.9*)			7.22–6.86 (m)	4.33 (dsept, 6.6, *1.9*), 1.10/1.07 (d, 6.6)
6a, A	8.17 (d, 2.1), *c*	6.59 (dd, *12.1*, 2.1)		7.89–6.87 (m)	3.96 (sept, 6.5), 1.22/0.80 (d, 6.5)
6a, B		6.35 (s, br)		7.89–6.87 (m)	3.96 (sept, 6.5), 1.29/0.75 (d, 6.5)
6c, A	7.98 (d, 1.9)	6.52 (dd, br *12.3*, 1.9)		2.77 (dd, *5.5*, 1.4)	3.86 (sept, 6.5), 1.23/0.75 (d, 6.5)
6c, B	*c*	6.22 (s, br)		1.76 (d, 1.2), 7.84–7.24 (m)	4.37 (sept, 6.5), 1.16/0.67 (d, 6.5)

[a] 100 MHz, $CDCl_3$, 293 K (unless stated otherwise), chemical shift values in ppm relative to Me_4Si. Suffixes to atoms refer to $R(CH)_\beta(CH)_\alpha(CH)_{im}NR'$, conform the numbering in the monoazadiene ligand system from which the compounds are derived. Italicized are the P–H coupling constants (Hz). [b] 100 MHz, toluene-d_8, 293 K. [c] Resonance masked by the Ph resonances.

Table VI. ^{13}C-NMR Data for $Ru(CO)_2(PPh_3)\{\eta^4$-RC(H)=C(H)C(H)=NR'$\}$ (**2a,b**), $Ru_2(CO)_4(PPh_3)_2\{C(H)_2CC(H)C(H)=N^iPr\}$ (**3**), $Ru(CO)_2(PPh_3)\{^iPrN=C(H)C(H)=N^iPr\}$ (**4**), and $Ru(CO)_2(PPh_3)Cl\{RC=C(H)C(H)=NR'\}$ (**6a,6c**) (**a**, R = Ph, R' = ^{i}Pr; **b**, R = Ph, R' = *p*-Tol; **c**, R = Me, R' = ^{i}Pr)[a]

	C_{im}	C_α	C_β	R	R'	PPh_3	CO_{Ru}
2a[b]	109.7	75.4	60.2	142.0, 127.8, 124.3, 123.7	59.5, 26.8/25.5	134.2 (d, *40*), 132.6 (d, *11*), 127.6 (d, *10*), 129.1 (s)	200.6 (d, *6.5*), 199.7
2b[b]	104.9	78.3	61.8	142.6, 129.3, 128.7, 124.9	153.4, 125.3, 122.2, 129.7 20.8	134.2 (d, *40*), 133.5 (d, *11*), 128.7 (d, *10*), 130.2 (s)	201.2 (d, *7.5*), 199.2
3[c]	172.0	75.1	201.7 (d, *3.8*)	56.2	58.4, 24.3/21.7	136.7 (d, *39*), 136.0 (d, *38*), 133.5 (d, *12*),133.4 (d, *12*), 128.0 (d, *10*), 127.9 (d, *10*), 129.4 (s), 129.2 (d, *2*)	209.0 (d, *4.1*), 208.6 (dd, *5.2*), 206.5 (d, *6.3*), 205.3 (d, *10.0*)
4[d]	134.1			63.1(d, *3.8*), 25.8/25.6		137.1 (d, *39*), 132.9 (d, *11*) 128.7 (d, *10*), 129.8 (d, *2*)	213.4 (d, *5.9*)
6a,[c] **A**	172.0 (d, *7.8*)	*e*	211.4 (d, *76*)	150.7, 127.21, 25.7, 128.2	59.4 (d, *4.9*), 24.8/22.8	134.6–128.4 (m)	197.8 (d, *7.6*), 194.0 (d, *6.3*)
6a, B	167.2	*e*	209.2 (d, *9.1*)	149.7, 127.1, 125.6, 128.1	54.0, 26.0/20.9	134.6–128.4 (m)	200.8 (d, *16.6*), 191.6 (d, *98.9*)
6c,[b] **A**	171.7 (d, *7.7*)	*e*	14.5 (d, *75*)	34.4	59.4 (d, *4.7*), 24.8/22.3	134.3–128.4 (m)	198.4 (d, *6.5*), 194.1 (d, *6.0*)
6c, B	167.3	*e*	214.3 (d, *8.1*)	34.0	52.9, 25.6/21.1	134.3–128.4 (m)	200.2 (d, *16.8*), 190.7 (d, *97.2*)

[a] Chemical shift values in ppm relative to Me_4Si, P–C coupling constants (in Hz) are in italics. [b] 25.1 MHz, $CDCl_3$, 263 K. [c] 75.46 MHz, $CDCl_3$ 293 K. [d] 25.1 MHz, toluene-d_8, 263 K. [e] Resonances masked by the Ph resonances.

1, on the other hand, have been thoroughly investigated.[30] Substitution of PPh_3 (e.g. by another phosphine ligand) appeared to be the dominating process, followed by CO substitution. Fragmentation of **1** was found to be the slowest process.

The formation of $Ru(CO)_3(PPh_3)_2$ in the reaction of **1** with MAD, which must be due to an overall dissociation of PPh_3 in **1** followed by recombination of $Ru(CO)_3(PPh_3)$ and PPh_3, shows that PPh_3 dissociation is a process operating in reactions of **1** with MAD as well.

The formation of the "allyl–imine" complex **3** in the reaction of **1** with an excess of MAD **c** (R, R' = Me, ^{i}Pr) is not unexpected, because the all-carbonyl analogue has been observed previously in the reaction of excess **c** with $Ru_3(CO)_{12}$. The mechanism for the formation of **3** in Scheme I is proposed by analogy with that reaction.[5] There seems to be no reason why the hydride-intermediate **A** should not be formed for MAD **a** or **b**, because in the reaction of **a** with $Ru_3(CO)_{12}$ an analogous intermediate was observed, which under the reaction conditions dimerized with loss of H_2, resulting in the tetranuclear chain-complex $Ru_4(CO)_{10}\{PhC=C(H)C(H)=N^iPr\}_2$.[5] Probably the dimerization step is inhibited in the PPh_3-substituted compounds, due to the steric interactions of the PPh_3 ligands in the expected tetranuclear product. Hence, intermediate **A** for MAD **a,b** has no opportunity to rearrange to a stable product and probably decomposes, which accounts for the rather low yield of **2**. The reaction of **1** with ^{i}Pr-DAB proceeds with high efficiency, as the yield before isolation of the mononuclear complex $Ru(CO)_2(PPh_3)\{^i$Pr-DAB$\}$ (**4**) has been estimated to be nearly quantitative. The selective formation of a mononuclear product is in sharp contrast to the reaction of ^{i}Pr-DAB with $Ru_3(CO)_{12}$, where the first isolable product was found to be dinuclear.[31] Apparently, the PPh_3 ligands promote the fragmentation into mononuclear species, which might be caused by the large steric requirements of the bulky PPh_3 ligand in the expected dinuclear complex with a six-electron donating,

Scheme I. Proposed Mechanism for the formation of **3** by Analogy with the Proposed Mechanism of the Formation of the $Ru_2(CO)_6$ Analogue of **3**

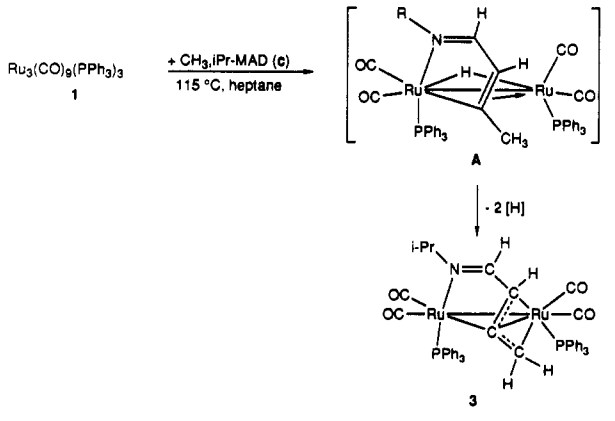

(30) Keaton, D. P.; Malik, Sher, K.; Poë, A. *J. Chem. Soc., Dalton Trans.* **1977**, 233.

(31) (a) Vrieze, K.; van Koten, G. *Inorg. Chim. Acta* **1985**, *100*, 79. (b) Vrieze, K. *J. Organomet. Chem.* **1986**, *300*, 307. (c) Mul, W. P.; Elsevier, C. J.; Frühauf, H.-W.; Vrieze, K.; Pein, I.; Zoutberg, M. C.; Stam, C. H. *Inorg. Chem.* **1990**, *29*, 2336.

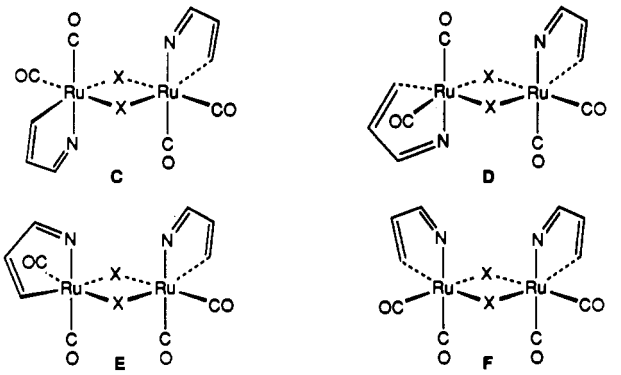

Figure 5. Four isomers of the Cl-bridged dimer, the parent compound for **6**.

bridging DAB ligand.[31] The yield of the mononuclear heterodiene product has also increased as compared to the reaction of **1** with MAD, which is probably caused by the better σ-donation properties of DAB and by the chelate effect exerted upon σ,σ-coordination of the DAB ligand.

The reactions of $Ru_3(CO)_9(PPh_3)_3$ (**1**) with the heterodienes MAD, DAB, and AOD show that **1**, in contrast to $Ru_3(CO)_{12}$, is an excellent precursor for the preparation of mononuclear Ru complexes of heterodienes.

Isomerization of 6. As outlined before, complex **6** exists as two isomers, **A** and **B** (Figure 3), and the ratio **A**:**B** appeared to be dependent on the method of preparation. In the thermal reaction (60 °C) of $[Ru(CO)_2Cl\{RC{=}C(H)C(H){=}N^iPr\}]_2$ with PPh_3, **6a** was formed as a mixture of the isomers **A** and **B** (ratio 1:3), while in the reaction at 25 °C isomer **A** was obtained selectively. This selectivity of the latter reaction is remarkable, because the parent complex $[Ru(CO)_2Cl\{RC{=}C(H)C(H){=}N^iPr\}]_2$ exists as a mixture of the four isomers which are depicted in Figure 5.

Due to the large trans effect of C_β it is reasonable that PPh_3 opens the Cl bridge by breaking of the Ru–Cl bond trans to C_β at one side of the dimer. In the case of the dimers **C** and **E**, the other side of the dimer will end up with a five-coordinate fragment with an open site trans to C_β, so these can react in a straightforward manner with another equivalent of PPh_3 to give **6a** (**A**) selectively. After bridge opening by 1 equiv of PPh_3 in the case of the dimers **D** and **F**, the open site will be located in trans position to a CO ligand and the reaction with a second molecule of PPh_3 would be expected to lead to the formation of **6a** (**B**), which has, however, not been observed. Apparently, the open site trans to CO is sterically shielded by the monoazadienyl ligand, so that this reaction with PPh_3 will be prohibited at room temperature. Instead, isomerization of the five-coordinate fragment may take place, yielding the sterically more favorable isomer, i.e. with PPh_3 trans to C_β. The finding that in the case of the sterically less demanding Me substituent on MAD-yl (as in **6c**) isomer **B** is indeed formed in small amounts at room temperature is in favor of the steric argument.

Complex **6a** (**A**) could be partly isomerized (25%) to isomer **B** in a thermal reaction (100 °C) during 2 h, indicating that isomer **B** is the thermodynamically favorable isomer. This is reasonable, because the strong donor ligand PPh_3 is now in trans position to the best acceptor ligand, i.e. CO. The isomerization process may occur via dissociation and re-association of a ligand. The coordinatively unsaturated intermediate can be formed in principle by dissociation of CO, PPh_3, or the N-atom. Support for the latter two activation types has been delivered by the byproducts in the reaction, viz. $Ru(CO)(PPh_3)_2Cl$(MAD-yl) and $Ru_2(PPh_3)_2Cl_2(CO)_4$, respectively.

One of the reasons that we decided to synthesize complex **6** was to study its reactivity with $NaBH_4$, aiming at the hydride analogue of **6**. The latter is interesting with respect to its stability in relation with the possibility to give reductive elimination. This subject will be discussed below.

Scheme II. Coordination and Cyclometalation Properties of MAD toward Fe- and Ru–Carbonyl Fragments

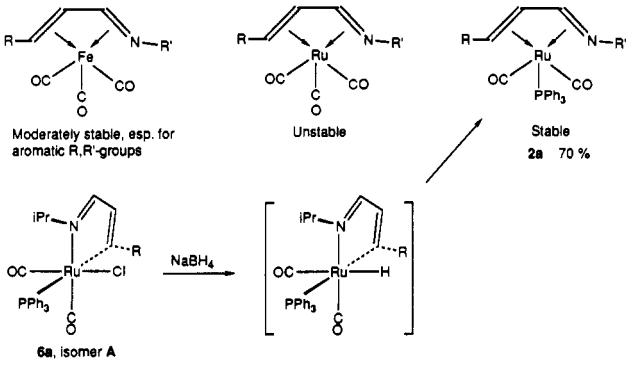

Bonding Properties of Mononuclear MAD(-yl) Complexes of Fe and Ru. As described in the introduction the properties of Fe– and Ru–carbonyl fragments with respect to the coordination strength of MAD and the tendency to give cyclometalation differ considerably. The most important aspects have been summarized in Scheme II. A comparison of the stability of the π,π-complexes shows that the $Fe(CO)_3$ complex is moderately stable, especially in the case of aromatic substituted MAD ligands. The $Ru(CO)_3$ complex is extremely unstable, as the ligand is easily replaced by CO. Complex **2**, $Ru(CO)_2(PPh_3)$\{MAD\}, on the contrary is very stable, and the MAD ligand cannot be substituted by CO at 100 °C (1 h). These features can be explained by taking into account the relative energies of the frontier orbitals of the metal fragments and of MAD. Substitution of CO in the $Ru(CO)_3$ fragment by PPh_3 induces an increase of electron density at Ru (e.g. expressed in the lower CO frequencies in IR) and a consequent rising in energy of the HOMO of the metal fragment. A similar effect is brought about when replacing Ru by Fe.[32,33] Apparently, a higher energy of the HOMO of the metal fragment results in more stable MAD complexes, which can be rationalized by considering π-back-bonding as the most important bonding interaction. The stabilizing effect of aromatic substituents observed in the $Fe(CO)_3$ complexes, thus lowering the LUMO of the ligand, is in agreement with this conclusion.

A final remark concerns the theoretical cyclometalation product of MAD on a $Ru(CO)_2(PPh_3)$ fragment, i.e. $HRu(CO)_2(PPh_3)$-(MAD-yl) (Scheme II). Undoubtedly, this complex is present in situ during the reaction of **6a** (**A**) with $NaBH_4$ but it gives rise to an instantaneous reductive elimination reaction, leading to **2a** in good yields. In the case of the isoelectronic metal fragment $Ir(PR_3)_2Cl$, cyclometalation of MAD has been observed to give the hydrido species $HIr(PR_3)_2Cl$(MAD-yl),[2] which is a stable product. Apparently, the cyclometalation process of MAD on $Ru(CO)_2(PPh_3)$ fragments is thermodynamically unfavorable.

Acknowledgment. We thank Prof. K. Vrieze for his interest and A. J. M. Duisenberg for the X-ray data collection. The crystallographic part of this work (W.J.J.S and A.L.S) was supported by the Netherlands Foundation for Chemical Research (SON) with financial aid from the Netherlands Organization for Scientific Research (NWO).

Supplementary Material Available: A thermal motion ellipsoid plot and tables of crystal data and details of the structure determination, fractional coordinates and isotropic thermal parameters of the hydrogen atoms, anisotropic thermal parameters of the non-hydrogen atoms, and all bond distances and angles for **2b** (7 pages). Ordering information is given on any current masthead page.

(32) Ziegler, T.; Tschinke, V.; Ursenbach, C. *J. Am. Chem. Soc.* **1987**, *109*, 4825.

(33) Beers, O. C. P.; Elsevier, C. J.; Vrieze, K.; Smeets, W. J. J.; Spek, A. L. *Organometallics*, in press.